

Growth and characterization of superconducting $Ca_{1-x}Na_xFe_2As_2$ single crystals by NaAs-flux method

Hong-Lin Zhou(周宏霖), Yu-Hao Zhang(张与豪), Yang Li(李阳), Shi-Liang Li(李世亮), Wen-Shan Hong(洪文山), and Hui-Qian Luo(罗会仟)

Citation: Chin. Phys. B, 2022, 31 (**11**): 117401. DOI: 10.1088/1674-1056/ac834a

What follows is a list of articles you may be interested in

Josephson vortices and intrinsic Josephson junctions in the layered iron-based superconductor $Ca_{10}(Pt_3As_8)((Fe_{0.9}Pt_{0.1})_2As_2)_5$

Qiang-Tao Sui(随强涛) and Xiang-Gang Qui(邱祥冈)

Chin. Phys. B, 2022, 31 (**9**): 097403. DOI: 10.1088/1674-1056/ac76ae

Raman phonon anomalies in $Sr(Fe_{1-x}Co_x)_2As_2$

Yanxing Yang(杨彦兴), Hewei Zhang(张鹤巍), and Haizheng Zhuang(庄海正)

Chin. Phys. B, 2022, 31 (**2**): 027401. DOI: 10.1088/1674-1056/ac0cd6

Superconductivity in octagraphene

Jun Li(李军) and Dao-Xin Yao(姚道新)

Chin. Phys. B, 2022, 31 (**1**): 017403. DOI: 10.1088/1674-1056/ac40fa

Revealing the A_{1g}-type strain effect on superconductivity and nematicity in FeSe thin flake

Zhaohui Cheng(程朝晖), Bin Lei(雷彬), Xigang Luo(罗习刚), Jianjun Ying(应剑俊), Zhenyu Wang(王震宇), Tao Wu(吴涛), and Xianhui Chen(陈仙辉)

Chin. Phys. B, 2021, 30 (**9**): 097403. DOI: 10.1088/1674-1056/ac1efa

Anomalous spectral weight transfer in the nematic state of iron-selenide superconductor

C Cai(蔡淙), T T Han(韩婷婷), Z G Wang(王政国), L Chen(陈磊), Y D Wang(王宇迪), Z M Xin(信子鸣), M W Ma(马明伟), Yuan Li(李源), Y Zhang(张焱)

Chin. Phys. B, 2020, 29 (**7**): 077401. DOI: 10.1088/1674-1056/ab90ec

---

Growth and characterization of superconducting $Ca_{1-x}Na_xFe_2As_2$ single crystals by NaAs-flux method

Hong-Lin Zhou(周宏霖)[1,2,†], Yu-Hao Zhang(张与豪)[3,†], Yang Li(李阳)[1,2], Shi-Liang Li(李世亮)[1,2,4], Wen-Shan Hong(洪文山)[1,2,5,‡], and Hui-Qian Luo(罗会仟)[1,4,§]

[1] *Beijing National Laboratory for Condensed Matter Physics, Institute of Physics, Chinese Academy of Sciences, Beijing* 100190, *China*
[2] *University of Chinese Academy of Sciences, Beijing* 100049, *China*
[3] *School of Advanced Engineering, University of Science and Technology Beijing, Beijing* 100083, *China*
[4] *Songshan Lake Materials Laboratory, Dongguan* 523808, *China*
[5] *International Center for Quantum Materials, School of Physics, Peking University, Beijing* 100871, *China*

(Received 23 June 2022; revised manuscript received 12 July 2022; accepted manuscript online 22 July 2022)

High-quality superconducting $Ca_{1-x}Na_xFe_2As_2$ single crystals have been successfully grown by the NaAs-flux method, with sodium doping level $x = 0.4$–0.64. The typical sizes of these crystals are more than 10 mm in *ab*-plane and ~ 0.1 mm along *c*-axis in thickness. X-ray diffraction, resistance and magnetization measurements are carried out to characterize the quality of these crystals. While no signature of magnetic phase transitions is detected in the normal state, bulk superconductivity is found for these samples, with a sharp transition at T_c ranging from 19.8 K ($x = 0.4$) to 34.8 K ($x = 0.64$). The doping dependences of the *c*-axis parameter and T_c are consistent with previous reports, suggesting a possible connection between the lattice parameters and superconductivity.

Keywords: iron-based superconductors, crystal growth, flux method

PACS: 74.25.–q, 74.25.Dw, 74.70.–b, 74.25.F– **DOI:** 10.1088/1674-1056/ac834a

1. Introduction

Unconventional superconductivity emerges either from stoichiometric or doped cuprates, nickelates, pnictides, and chalcogenides,[1–6] or from pressure tuned heavy fermion compounds, Cr-based and Mn-based compounds.[7–12] It is a great challenge to reveal the microscopic mechanism of superconductivity in these materials due to various phases coexisting or competing with each other.[3,5] To achieve such a goal, high quality crystals are certainly essential for the exploration of those complex interactions among electrons and atoms.[12–22] For iron arsenide superconductors, the crystal growth methods are quite limited due to the highly toxic arsenic vapor.[23] Usually, the iron arsenide crystals are grown by flux methods in sealed quartz tubes, where the flux could be NaCl/KCl mixture, Sn, FeAs, NaF, CaAs, NaAs, KAs, etc.[24–53] At the early stage, the 1111-type iron-based superconductor (FeSC) $LaFeAsO_{1-x}F_x$ were grown by NaCl/KCl flux,[24–26] and the obtained crystals with several micrometer sizes are only suitable for transport measurements.[27,28] Later, the 122-type FeSCs are grown by Sn flux or FeAs self-flux methods, which significantly improve the sample sizes to centimeter scale but probably with some impurity phases.[29–35] Similar grown applications are successful in other systems such as 111-type, 112-type, and 1144-type FeSCs.[36–43] After that, the NaF, CaAs, NaAs, KAs fluxes with lower melting points are demonstrated to be very useful to grow the 1111-type FeSCs as well as other systems.[44–49] In particular, the hole-like 12422-type systems and the hoped-doped 122-type FeSCs grown by NaAs or KAs show very homogeneous quality and bulk superconductivity.[50–55]

The 122-type FeSCs are the most extensively studied systems due to available crystals with high quality and large sizes.[14–17] The parent compound of the '122' families is typically in the form of $AeFe_2As_2$ (Ae = alkaline earth metal, *e.g.*, Ca, Sr, Ba), exhibiting both antiferromagnetic (AF) and structural phase transitions from 138 K to 203 K.[56–59] Superconductivity can be induced by hole (*e.g.*, Na and K), electron (*e.g.*, Ni, Co, Cu, Rh, Ir, Pd, La, Ce, and Pr), or isovalent (*e.g.*, P and Ru) dopings on the alkaline earth metal, iron, and arsenic sites, respectively.[60–77] While the FeAs self-flux method can produce high quality crystals for those electron doped compounds throughout the phase diagram, homogeneous and tunable superconductivity in the hole doped compounds is still a challenge.[33–35,54,55] The 122-type FeSCs generally host a phase diagram with competing AF order and superconductivity similar to cuprates, but the details of the phase diagram strongly depend on the alkaline earth metal and the doped elements.[14,15] For example, in the electron doped systems such as $Ba(Fe_{1-x}Ni_x)_2As_2$ or $Ba(Fe_{1-x}Co_x)_2As_2$, the long-range stripe-type AF order in the orthorhombic lattice is gradually suppressed

[†] These authors contributed equally to this work.
[‡] Corresponding author. E-mail: wenshanhong@pku.edu.cn
[§] Corresponding author. E-mail: hqluo@iphy.ac.cn

© 2022 Chinese Physical Society and IOP Publishing Ltd

and degenerates to a short-range order finally disappearing above T_c near the optimal doping level.[78–81] The cases become more complicated in the hole doped systems, such as $Ba_{1-x}K_xFe_2As_2$,[82] $Ba_{1-x}Na_xFe_2As_2$,[83,84] $Sr_{1-x}Na_xFe_2As_2$,[85,86] and $Ca_{1-x}Na_xFe_2As_2$,[87] a tetragonal magnetic phase (so-called C_4 phase) with ordered moments along c-axis is revealed to competing with the orthorhombic magnetic phase (so-called C_2 phase) just before the optimal doping level in the underdoped region, the C_2 phase may reentry at low temperature in $Ba_{1-x}K_xFe_2As_2$ and $Ca_{1-x}Na_xFe_2As_2$.[82,87] Moreover, the superconducting dome for the same doped element is significantly distinct among Ba-, Sr-, and Ca-122 systems. Like say, the maximum T_c = 30–35 K locates at $x = 0.4$, 0.55, and 0.75 for $Ba_{1-x}Na_xFe_2As_2$, $Sr_{1-x}Na_xFe_2As_2$, $Ca_{1-x}Na_xFe_2As_2$, respectively.[84–89] The Ca-122 compounds show a unique collapse tetragonal phase where both the AF fluctuations and superconductivity may be absent.[90–93] All these facts suggest that the chemical doping induced changes on the local crystalline structure are crucial to the electronic ground states in FeSCs besides the charge carrier concentration. Thus, further investigations on this issue are highly desired to understand the unconventional superconductivity in FeSCs, counting on high-quality and sizeable single crystals.

In this paper, we report a method to grow sizeable and homogenous $Ca_{1-x}Na_xFe_2As_2$ single crystals with doping level from $x = 0.4$ to $x = 0.64$. While AF order is absent in these batches of crystals, bulk superconductivity is found with transition temperatures ranging from $T_c = 20$ K in the $x = 0.4$ sample to $T_c = 34.5$ K in the optimally doped $x = 0.64$ sample. Compared to the FeAs self-flux method, this NaAs self-flux method is quite hard to reach the very underdoped level in $Ca_{1-x}Na_xFe_2As_2$. We summarize the results of $Ca_{1-x}Na_xFe_2As_2$ in the literature and compare with the $Ba_{1-x}K_xFe_2As_2$ system from underdoped region to optimal doping level. A linear dependence of c-axis parameter and a parabolic dependence of T_c versus the doping level x are found, respectively, suggesting a quantitative connection between the local crystalline structure and the unconventional superconductivity in FeSCs.

2. Experimental details

We used NaAs as flux to grow the $Ca_{1-x}Na_xFe_2As_2$ single crystals. Firstly, three precursors NaAs, CaAs and Fe_2As were prepared with highly pure raw materials Na($> 99.5\%$), Ca($> 99.9\%$), Fe($> 99.5\%$) and As($> 99.99\%$) by the solid state reaction method in evacuated and sealed quartz tubes. NaAs was synthesized by mixing many small pieces of Na and As powders and reacting at 400 °C for 20 h. CaAs was prepared by mixing Ca grains and As powders and reacting at 400 °C for 20 h then keeping at 630 °C for another 20 h. Fe_2As was synthesized by reacting the mixture of Fe and As powders at 500 °C for 10 h then at 700 °C for another 10 h. All heating process should be very carefully and gently under a rate less than 20 °C/h, to avoid the danger from vapor of these raw materials. Secondly, these three precursors were mixed together at a molar ratio of CaAs : Fe_2As : NaAs = $(1-x) : 1 : (x+3)$ to grow $Ca_{1-x}Na_xFe_2As_2$ single crystals. After grinding for about 30 min, the mixture was loaded in an alumina crucible and then sealed under argon atmosphere in an Nb tube, this tube was further sealed in an evacuated quartz ampoule. Thirdly, the sealed mixture was placed in a box furnace and slowly heated up to 600 °C and kept warm for 5 h to fully melt the NaAs flux, it was then heated to 980 °C at a rate of 0.76 °C/min, and to 1150 °C at a rate of 0.425 °C/min, hold for 24 h to melt the CaAs (melting point about 650 °C) and Fe_2As (melting point about 930 °C) materials, followed by slowly cooling down to 650 °C at a rate of 2 °C/h to grow the crystals. Finally, the electricity of the furnace was turned off to cool down the mixture to room temperature naturally, until it is safe to fetch out. Large pieces of $Ca_{1-x}Na_xFe_2As_2$ single crystals were obtained after crashing the tubes and cleaning the NaAs flux. Residual NaAs flux on the crystal surface can be fully dissolved in the deionized water.

The crystal surface morphology and distribution of elements were examined by a scanning electron microscope (SEM) equipped with energy dispersive x-ray (EDX) analyzer. The chemical compositions of our crystals were determined by the inductively coupled plasma (ICP) analysis. The crystalline quality and doping effects on the lattice parameters were checked by single-crystal x-ray diffraction (XRD) on a 9 kW high-resolution diffraction system (SmartLab) with Cu K_α radiation ($\lambda = 1.5406$ Å) at room temperature in the reflection mode, with 2θ ranging from 10° to 65°. The Laue pattern was collected by an x-ray Laue camera (Photonic Sciences) in backscattering mode with incident beam along c-axis. The resistivity was measured by the standard four-probe method in a physical property measurement system (Quantum Design-PPMS). The DC-magnetic susceptibility was measured with the zero-field-cooling (ZFC) method and a small field H = 3 Oe in parallel c-axis in a magnetic property measurement system (Quantum Design-MPMS).

3. Results and discussion

We have successfully grown 5 batches of $Ca_{1-x}Na_xFe_2As_2$ single crystals with nominal doping $x = 0.3$, 0.4, 0.5, 0.6, 0.7. The actual doping concentration x' is determined by the ICP method and listed in Table 1, where the relative errors are about 5% as estimated from the analyses on several pieces of crystals. Due to the excess NaAs precursor as the flux in the mixture, even a small nominal x could result in significant actual dopings, giving $x' = 0.2 + 0.64x$.

Such effect hampers us to reach low doping level in the underdoped region in comparison to the FeAs-flux method.[33,94,95] For high doping levels, the Na concentration seems to reach a saturation point in this method. So far, overdoped $Ca_{1-x}Na_xFe_2As_2$ crystals are still very hard to obtain, but overdoped $Ba_{1-x}K_xFe_2As_2$ including KFe_2As_2 can be grown by the KAs-flux method.[54,55,96,97] In the following, we use the actual doping level to refer to our samples. The homogeneity of our crystals is examined by SEM and EDX analyses, the results of three typical dopings $x = 0.40$, 0.44, and 0.64 are shown in Fig. 1. The SEM photos show flat surfaces with some crack edges from different layers. EDX analyses on four elements all exhibit homogenous distributions.

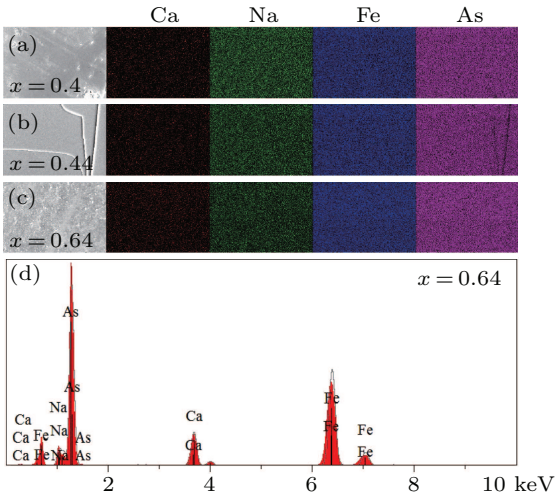


Fig. 1. (a)–(c) SEM photos of the cleaved surfaces and element distribution analyses for $Ca_{1-x}Na_xFe_2As_2$ (x =0.40, 0.44 and 0.64) crystals. (b) A typical EDX spectrum for one single crystal with $x = 0.64$.

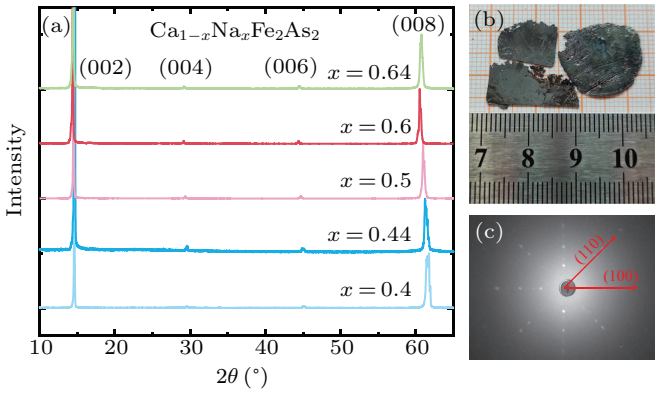


Fig. 2. (a) The x-ray diffraction patterns at room temperature for $Ca_{1-x}Na_xFe_2As_2$ single crystals. (b) A photo of $Ca_{0.6}Na_{0.4}Fe_2As_2$ platy monocrystal. (c) Typical Laue reflection at room temperature for our crystals.

The crystalline quality is checked by x-ray diffraction and presented in Fig. 2. Figure 2(a) shows the XRD patterns with the incident beam along the c-axis of our crystals. All diffraction peaks indexed as $(0,0,l)$ (l = even) are sharp and no diffraction from impurity phases is observed. With the increase of Na doping, the 2θ of the last peak shifts to low angle side, suggesting increasing c-axis lattice parameter. We have calculated the c-axis parameter by fitting the peak positions and listed in Table 1. The photo in Fig. 2(b) shows the typical sizes of our $Ca_{1-x}Na_xFe_2As_2$ single crystals. The dimensions of the largest crystal are about 17 mm × 16 mm × 0.5 mm. The cleaved surface is shiny under the light, and the texture is brittle. The Laue reflection in ab-plane for $Ca_{0.36}Na_{0.64}Fe_2As_2$ is shown in Fig. 2(c). Again, the bright and sharp scattering spots indicate the high quality of this sample, clear orientations along [1,0,0] and [1,1,0] of the crystal can be easily identified.

Table 1. Doping concentrations, c-axis parameter, and T_c of our $Ca_{1-x}Na_xFe_2As_2$ single crystals.

Nominal x	Actual x	c-axis lattice constant (Å)	T_c (K)
0.3	0.40	12.03	19.8
0.4	0.44	12.11	21.9
0.5	0.50	12.13	29.3
0.6	0.60	12.22	34.5
0.7	0.64	12.18	34.8

Figure 3(a) shows the electrical resistance in ab-plane under zero field as a function of temperature. We normalize them by the resistance at 300 K for comparison, all of them show a smooth evolution in the normal state and a sharp superconducting transition at T_c. To search for the signature of any magnetic transitions, we plot the first-order derivative of the resistance versus temperature in the inset of Fig. 3(a). Only a narrow peak corresponding to the superconducting transition can be identified, the value of T_c for each doping is listed in Table 1, too. Therefore, for all samples with actual doing $x = 0.40$–0.64, they are paramagnetic in the normal state, which is consistent with the previous reports on polycrystalline samples.[82,87] We also notice that the residual resistance just above T_c is less than 10 % of the room temperature resistance, giving a large residual resistivity ratio RRR ≈ 10. Such large RRR also confirms the high quality of our crystals. For references, RRR is about 5 for optimally hole-doped $Ba_{1-x}K_xFe_2As_2$,[33] and about 2 for optimally electron-doped $Ba(Fe_{1-x}Ni_x)_2As_2$.[34] For high pure KFe_2As_2 grown by KAs flux, RRR can be over than 2000.[96,97] The superconducting volume of these $Ca_{1-x}Na_xFe_2As_2$ crystals was measured by magnetization under a magnetic field of 3 Oe along c-axis in ZFC mode. We only checked three typical samples with $x = 0.40$, 0.44, and 0.64 as shown in Fig. 3(b). All of them show sharp superconducting transitions with a strong diamagnetic signal and a narrow width $\Delta T < 2$ K. The magnetic susceptibility $4\pi\chi = -1$ at low temperatures indicate the full Meissner state, namely bulk superconductivity in these samples. In the parent compound $CaFe_2As_2$, a magnetic transition with stripe-type order can be probed at about $T_N = 170$ K by the magnetization under high field, which shows a deletion below T_N and a linear temperature dependence above T_N.[14,58] However, the normal state resistance is more sensitive to the

magnetic/structural transitions in FeSCs,[33–36] thus we do not have to measure the magnetization up to high temperatures to further search the magnetic order.

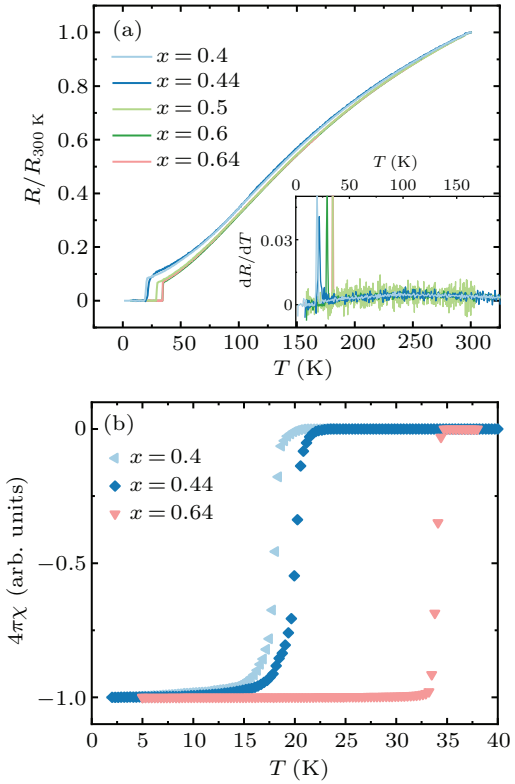


Fig. 3. (a) The temperature dependence of resistance for $Ca_{1-x}Na_xFe_2As_2$ crystals. All data are normalized by the room temperature resistance. The inset shows the first-order derivative of the resistance. (b) Magnetization measured under ZFC mode for three typical dopings $x = 0.40$, 0.44, 0.64.

Finally, we compare the doping dependence of the c-axis parameter and superconducting transition T_c with the previous reports on $Ca_{1-x}Na_xFe_2As_2$.[75–77,87,89] As shown in Fig. 4, our results can merge well with previous reports for both parameters. In Fig. 4(a), we also plot the doping dependence of the c-axis parameter in $Ba_{1-x}K_xFe_2As_2$.[33,95] As we can see, for both hole doped systems, the c-axis lattice is continuously stretched by chemical substitutions, as the radius of alkali metal is larger than alkali earth metal.[98,99] The c-axis has a linear relationship with doping level x in the underdoped regime: $c = 0.78x + 11.7$ for $Ca_{1-x}Na_xFe_2As_2$ and $c = 0.88x + 12.98$ for $Ba_{1-x}K_xFe_2As_2$,[95,98,99] with similar slopes. With those T_c of $Ca_{1-x}Na_xFe_2As_2$ summarized in Fig. 4(b),[75–77,87,89] we can roughly fit by a parabolic function: $T_c = -155.2x^2 + 227.18x - 48.89$. Such a relation probably suggests that the superconducting behavior in the underdoped region is also strongly related to the d-spacing between Fe-As layers. Particularly, for those systems with smaller c-axis parameters thus closer distance of the adjacent Fe–As layers, the inter Fe–As layer coupling is stronger, thus to reach the optimal superconductivity upon doping requires higher concentration. This naturally explains the increasing doping to the optimal level in $(Ba,Sr,Ca)_{1-x}Na_xFe_2As_2$ systems, where their parent compounds $(Ba,Sr,Ca)Fe_2As_2$ have decreasing c-axis: $c = 13.04$, 12.37, 11.75 Å at room temperature, respectively.[84–89] For the overdoped region, although the c-axis continuously increasing upon doping, strong mismatches of the Fermi surface sizes are expected to suppress the superconducting pairing.[5] It was proposed in Ref. [100] that T_c is higher when the pnictogen height and As–Fe–As bond angle more close to form a regular tetrahedron among many systems of FeSCs. This could be a consequence from competing interactions strongly associated with the local crystalline structure.

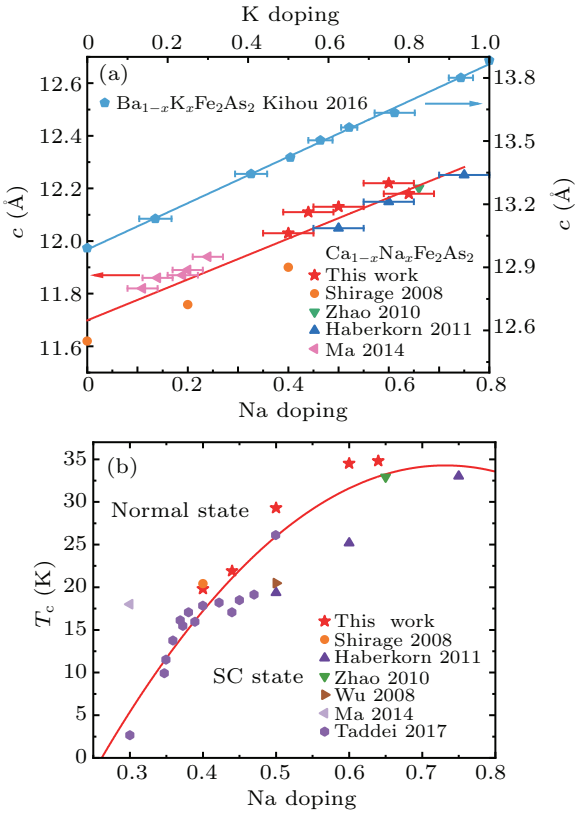


Fig. 4. (a) Doping dependence of the c-axis parameters in the $Ca_{1-x}Na_xFe_2As_2$ system[75–77,87,89] in comparison with the $Ba_{1-x}K_xFe_2As_2$ system.[33,95,98,99] Here the relative errors for the chemical compositions of our sample are about 5% from the ICP measurements, errors for other samples are obtained from the above-mentioned literature, and the solid lines are linear fittings. (b) Summary of the doping dependence of T_c in $Ca_{1-x}Na_xFe_2As_2$.[75–77,87,89] The solid line is a parabolic fitting to all data.

4. Summary

In summary, we have successfully grown a series of large $Ca_{1-x}Na_xFe_2As_2$ single crystals with actual Na doping $x =$ 0.4–0.64 using the NaAs-flux method. These crystals show bulk superconductivity but no magnetic transitions. The positive doping dependences both for T_c and c-axis lattice parameter suggest that they are probably related. These homogeneous and sizable crystals provide us chances to further investigate the unconventional superconductivity in FeSCs, especially for those techniques requiring large crystals, such as inelastic neutron scattering and μSR.

Acknowledgements

The authors thank Professor Xing-Ye Lu, Dr. Zhen Tao, Dr. Li-Hong Yang, Dr. Jie Li and Mr. Wei-Wen Huang for assistance in sample characterization.

Project supported by the National Key Research and Development Program of China (Grant No. 2018YFA0704200), the National Natural Science Foundation of China (Grant Nos. 11822411 and 11961160699), the Strategic Priority Research Program (B) of the CAS (Grants Nos. XDB25000000 and XDB33000000), the K. C. Wong Education Foundation (Grant No. GJTD-2020-01), the Youth Innovation Promotion Association of CAS (Grant No. Y202001), the Postdoctoral Innovative Talent program (Grant No. BX2021018), and the China Postdoctoral Science Foundation (Grant No. 2021M700250).

References

[1] Lee P A, Nagaosa N and Wen X G 2006 *Rev. Mod. Phys.* **78** 17
[2] Gu Q and Wen H H 2022 *The Innovation* **3** 100202
[3] Zhou X, Lee W S, Imada M, Trivedi N, Phillips P, Kee H Y, Törmä P and Eremets M 2021 *Nat. Rev. Phys.* **3** 462
[4] Chen X H, Dai P, Feng D, Xiang T and Zhang F 2014 *Nat. Sci. Rev.* **1** 371
[5] Si Q, Yu R and Abrahams E 2016 *Nat. Rev. Mater.* **1** 16017
[6] Kamihara Y, Watanabe T, Hirano M and Hosono H 2008 *J. Am. Chem. Soc.* **130** 3296
[7] White B D, Thompson J D and Maple M B 2015 *Physica C* **514** 246
[8] Wu W, Zhang X D, Yin Z H, Zheng P, Wang N L and Luo J L 2010 *Sci. China Phys. Mech. Astron.* **53** 1207
[9] Wu W, Cheng J G, Matsubayashi K, Kong P P, Lin F K, Jin C Q, Wang N L, Uwatoko Y and Luo J L 2014 *Nat. Commun.* **5** 5508
[10] Cheng J G, Matsubayashi K, Wu W, Sun J P, Lin F K, Luo J L and Uwatoko Y 2015 *Phys. Rev. Lett.* **114** 117001
[11] Liu Z Y, Dong Q X, Yang P T, Shan P F, Wang B S, Sun J P, Dun Z L, Uwatoko Y, Chen G F, Dong X L, Zhao Z X and Cheng J G 2022 *Phys. Rev. Lett.* **128** 187001
[12] Yang P T, Dong Q X, Shan P F, Liu Z Y, Sun J P, Dun Z L, Uwatoko Y, Chen G F, Wang B S and Cheng J G 2022 *Chin. Phys. Lett.* **39** 067401
[13] Tranquada J M, Xu G and Zaliznyak I A 2014 *J. Magn. Magn. Mater.* **350** 148
[14] Stewart G R 2011 *Rev. Mod. Phys.* **83** 1589
[15] Dai P 2015 *Rev. Mod. Phys.* **87** 855
[16] Gong D and Luo H 2018 *Acta Phys. Sin.* **67** 207407 (in Chinese)
[17] Luo H Q 2017 *Chin. Sci. Bull.* **62** 3955
[18] Gong D *et al.* 2022 *Front. Phys.* **10** 886459
[19] Wen J S, Xu G Y, Gu G D, Tranquada J M and Birgeneau R J 2011 *Rep. Prog. Phys.* **74** 124503
[20] Jiang H, Sun Y L, Xu Z A and Cao G H 2013 *Chin. Phys. B* **22** 087410
[21] Xie T, Liu C, Fennell T, Stuhr U, Li S L and Luo H Q 2021 *Chin. Phys. B* **30** 127402
[22] Zhang C *et al.* 2022 *Sci. China Phys. Mech. Astron.* **65** 237411
[23] Hosono H and Kuroki K 2015 *Physica C* **514** 399
[24] Quebe P, Terbüchte L J and Jeitschko W 2000 *J. Alloys Compounds* **302** 70
[25] Zhigadlo N D, Katrych S, Bukowski Z and Karpinski J 2008 *J. Phys.: Condens. Matter* **20** 342202
[26] Fang L, Cheng P, Jia Y, Zhu X Y, Luo H Q, Mu G, Gu C Z and Wen H H *J. Cryst. Growth* **311** 358
[27] Jia Y, Cheng P, Fang L, Luo H Q, Yang H, Ren C, Shan L, Gu C Z and Wen H H 2008 *Appl. Phys. Lett.* **93** 032503
[28] Luo H Q, Cheng P, Wang Z S, Yang H, Jia Y, Fang L, Ren C, Shan L and Wen H H 2009 *Physica C* **469** 477
[29] Ni N, Bud'ko S L, Kreyssig A, Nandi S, Rustan G E, Goldman A I, Gupta S, Corbett J D, Kracher A and Canfield P C 2008 *Phys. Rev. B* **78** 014507
[30] Chen G F, Li Z, Dong J, Li G, Hu W Z, Zhang X D, Song X H, Zheng P, Wang N L and Luo J L 2008 *Phys. Rev. B* **78** 224512
[31] Ronning F, Klimczuk T, Bauer E D, Volz H and Thompson J D 2008 *J. Phys.: Condens. Matter* **20** 322201
[32] Yan J Q *et al.* 2008 *Phys. Rev. B* **78** 024516
[33] Luo H, Wang Z, Yang H, Cheng P, Zhu X and Wen H H 2008 *Supercond. Sci. Technol.* **21** 125014
[34] Chen Y, Lu X, Wang M, Luo H and Li S 2011 *Supercond. Sci. Technol.* **24** 065004
[35] Zhang R, Gong D, Lu X, Li S, Dai P and Luo H 2014 *Supercond. Sci. Technol.* **27** 115003
[36] Chen G F, Hu W Z, Luo J L and Wang N L 2009 *Phys. Rev. Lett.* **102** 227004
[37] Wang M *et al.* 2011 *Phys. Rev. B* **83** 220515
[38] Xing X Z, Zhou W, Zhou N, Yuan F F, Pan Y Q, Zhao H J, Xu X F and Shi Z X 2016 *Supercond. Sci. Technol.* **29** 055005
[39] Xie T, Gong D, Zhang W, Gu Y, Huesges Z, Chen D, Liu Y, Hao L, Meng S, Lu Z, Li S and Luo H 2017 *Supercond. Sci. Technol.* **30** 095002
[40] Xie T, Gong D, Ghosh H, Ghosh A, Soda M, Masuda T, Itoh S, Bourdarot F, Regnault L P, Danilkin S, Li S and Luo H 2018 *Phys. Rev. Lett.* **120** 137001
[41] Luo X and Chen X 2015 *Sci. China Mater.* **58** 77
[42] Meier W R, Kong T, Bud'ko S L and Canfield P C 2017 *Phys. Rev. Mater.* **1** 013401
[43] Xie T, Wei Y, Gong D, Fennell T, Stuhr U, Kajimoto R, Ikeuchi K, Li S, Hu J and Luo H 2018 *Phys. Rev. Lett.* **120** 267003
[44] Yan J Q *et al.* 2015 *Phys. Rev. B* **91** 024501
[45] Iyo A, Kawashima K, Ishida S, Fujihisa H, Gotoh Y, Eisaki H and Yoshida Y 2018 *J. Am. Chem. Soc.* **140** 369
[46] Yan J Q *et al.* 2009 *Appl. Phys. Lett.* **95** 222504
[47] Yan J Q, Jensen B, Dennis K W, McCallum R W and Lograsso T A 2011 *Appl. Phys. Lett.* **98** 072504
[48] Ma Y H, Zhang H, Gao B, Hu K K, Ji Q C, Mu G, Huang F Q and Xie X M 2015 *Supercond. Sci. Technol.* **28** 085008
[49] Ma M W, Ruan B B, Zhou M H, Gu Y D, Yang Q S, Sun J N and Ren Z A 2022 *J. Cryst. Growth* **585** 126562
[50] Wang Z C, He C Y, Wu S Q, Tang Z T, Liu Y, Ablimit A, Feng C M and Cao G H 2016 *J. Am. Chem. Soc.* **138** 7856
[51] Wang Z C, He C Y, Tang Z T, Wu S Q and Cao G H 2017 *Sci. China Mater.* **60** 83
[52] Wang T, Chu J N, Feng J X, Wang L L, Xu X G, Li W, Wen H H, Liu X S and Mu G 2020 *Sci. China Phys. Mech. Astron.* **63** 297412
[53] Hong W, Song L, Liu B, Li Z, Zeng Z, Li Y, Wu D, Sui Q, Xie T, Danilkin S, Ghosh H, Ghosh A, Hu J, Zhao L, Zhou X, Qiu X, Li S and Luo H 2020 *Phys. Rev. Lett.* **125** 117002
[54] Yi X L, Li M, Xing X Z, Meng Y, Zhao C Y and Shi Z X 2020 *New J. Phys.* **22** 073007
[55] Liu Y, Tanatar M Z, Straszheim W E, Jensen B, Dennis K W, McCallum R W, Kogan V G, Prozorov R and Lograsso T A 2014 *Phys. Rev. B* **89** 134504
[56] Huang Q, Qiu Y, Bao W, Green M A, Lynn J W, Gasparovic Y C, Wu T, Wu G and Chen X H 2008 *Phys. Rev. Lett.* **101** 257003
[57] Krellner C, Caroca-Canales N, Jesche A, Rosner H, Ormeci A and Geibel C 2008 *Phys. Rev. B* **78** 100504
[58] Goldman A I, Argyriou D N, Ouladdiaf B, Chatterji T, Kreyssig A, Nandi S, Ni N, Bud'ko S L, Canfield P C and McQueeney R J 2008 *Phys. Rev. B* **78** 100506
[59] Gong D L, Liu Z Y, Gu Y H, Xie T, Ma X Y, Luo H Q, Yang Y F and Li S L 2017 *Phys. Rev. B* **96** 104514
[60] Rotter M, Tegel M and Johrendt D 2008 *Phys. Rev. Lett.* **101** 107006
[61] Goko T *et al.* 2009 *Phys. Rev. B* **80** 024508
[62] Zhao K, Liu Q Q, Wang X C, Deng Z, Lv Y X, Zhu J L, Li F Y and Jin C Q 2011 *Phys. Rev. B* **84** 184534
[63] Shinohara N, Tokiwa K, Fujihisa H, Gotoh Y, Ishida S, Kihou K, Lee C H, Eisaki H, Yoshida Y and Iyo A 2015 *Supercond. Sci. Technol.* **28** 062001
[64] Sefat A S, Jin R, McGuire M A, Sales B C, Singh D J and Mandrus D 2008 *Phys. Rev. Lett.* **101** 117004
[65] Li L J *et al.* 2009 *New J. Phys.* **11** 025008
[66] Ni N, Thaler A, Yan J Q, Kracher A, Colombier E, Bud'ko S L, Canfield P C and Hannahs S T 2010 *Phys. Rev. B* **82** 024519

[67] Canfield P C, Bud'ko S L, Ni N, Yan J Q and Kracher A 2009 *Phys. Rev. B* **80** 060501(R)
[68] Ni N, Thaler A, Kracher A, Yan J Q, Bud'ko S L and Canfield P C 2009 *Phys. Rev. B* **80** 024511
[69] Han F *et al.* 2009 *Phys. Rev. B* **80** 024506
[70] Kirshenbaum K, Saha S R, Drye T and Paglione J 2010 *Phys. Rev. B* **82** 144518
[71] Lv B, Deng L Z, Gooch M, Wei F Y, Sun Y Y, Meen J K, Xue Y Y, Lorenz B and Chu C W 2011 *Proc. Natl Acad. Sci. USA* **108** 15705
[72] Jiang S, Xing H, Xuan G F, Wang C, Ren Z, Feng C, Dai J H, Xu Z A and Cao G H 2009 *J. Phys.: Condens. Matter* **21** 382203
[73] Kasahara S, Shibauchi T, Hashimoto K, Ikada K, Tonegawa S, Okazaki R, Shishido H, Ikeda H, Takeya H, Hirata K, Terashima T and Matsuda 2010 *Phys. Rev. B* **81** 184519
[74] Thaler A, Ni N, Kracher A, Yan J Q, Bud'ko S L and Canfield P C 2010 *Phys. Rev. B* **82** 014534
[75] Shirage P M, Miyazawa K, Kito H, Eisaki H and Iyo A 2008 *Appl. Phys. Exp.* **1** 081702
[76] Zhao K, Liu Q Q, Wang X C, Deng Z, Lv Y X, Zhu J L, Li F Y and Jin C Q 2010 *J. Phys.: Condens. Matter* **22** 222203
[77] Ma J Q, Luo X G, Cheng P, Zhu N, Liu D Y, Chen F, Ying J J, Wang A F, Lu X F, Lei B and Chen X H 2014 *Phys. Rev. B* **85** 174512
[78] Pratt D K, Kim M G, Kreyssig A, Lee Y B, Tucker G S, Thaler A, Tian W, Zarestky J L, Bud'ko S L, Canfield P C, Harmon B N, Goldman A I and McQueeney R J 2011 *Phys. Rev. Lett.* **106** 257001
[79] Luo H Q, Zhang R, Laver M, Yamani Z, Wang M, Lu X Y, Wang M Y, Chen Y C, Li S L, Chang S, Lynn J W and Dai P C 2012 *Phys. Rev. Lett.* **108** 247002
[80] Kim M G, Lamsal J, Heitmann T W, Tucker G S, Pratt D K, Khan S N, Lee Y B, Alam A, Thaler A, Ni N, Ran S, Bud'ko S L, Marty K J, Lumsden M D, Canfield P C, Harmon B N, Johnson D D, Kreyssig A, McQueeney R J and Goldman A I 2012 *Phys. Rev. Lett.* **109** 167003
[81] Lu X Y, Gretarsson H, Zhang R, Liu X R, Luo H Q, Tian W, Laver M, Yamani Z, Kim Y J, Nevidomskyy A H, Si Q M and Dai P C 2013 *Phys. Rev. Lett.* **110** 257001
[82] Böhmer A. E, Hardy F, Wang L, Wolf T, Schweiss P and Meingast C 2015 *Nat. Commun.* **6** 7911
[83] Avci S, Chmaissem O, Allred J M, Rosenkranz S, Eremin I, Chubukov A V, Bugaris D E, Chung D Y, Kanatzidis M G, Castellan J P, Schlueter J A, Claus H, Khalyavin D D, Manuel P, Daoud Aladine A and Osborn R 2014 *Nat. Commun.* **5** 3845
[84] Wang L, Hardy F, Böhmer A E, Wolf T, Schweiss P and Meingast C 2016 *Phys. Rev. B* **93** 014514
[85] Allred J M *et al.* 2016 *Nat. Phys.* **12** 493
[86] Wu S *et al.* 2021 *Phys. Rev. Lett.* **126** 107001
[87] Taddei K M, Allred J M, Bugaris D E, Lapidus S H, Krogstad M J, Claus H, Chung D Y, Kanatzidis M G, Osborn R, Rosenkranz S and Chmaissem O 2017 *Phys. Rev. B* **95** 064508
[88] Taddei K M, Allred J M, Bugaris D E, Lapidus S H, Krogstad M J, Stadel R, Claus H, Chung D Y, Kanatzidis M G, Rosenkranz S, Osborn R and Chmaissem O 2016 *Phys. Rev. B* **93** 134510
[89] Haberkorn N, Maiorov B, Jaime M, Usov I, Miura M, Chen G F, Yu W and Civale L 2011 *Phys. Rev. B* **84** 064533
[90] Prokeš K, Kreyssig A, Ouladdiaf B, Pratt D K, Ni N, Bud'ko S L, Canfield P C, McQueeney R J, Argyriou D N and Goldman A I 2010 *Phys. Rev. B* **81** 180506
[91] Soh J H, Tucker G S, Pratt D K, Abernathy D L, Stone M B, Ran S, Bud'ko S L, Canfield P C, Kreyssig A, McQueeney R J and Goldman A I 2013 *Phys. Rev. Lett.* **111** 227002
[92] Ortenzi L, Gretarsson H, Kasahara S, Matsuda Y, Shibauchi T, Finkelstein K D, Wu W, Julian S R, Kim Y J, Mazin I I and Boeri L 2015 *Phys. Rev. Lett.* **114** 047001
[93] Su Y, Setty C, Wang Z and Hu J 2012 *Phys. Rev. B* **85** 184517
[94] Materne P, Kamusella S, Sarkar R, Goltz T, Spehling J, Maeter H, Harnagea L, Wurmehl S, Büchner B, Luetkens H, Timm C and Klauss H H *et al.* 2015 *Phys. Rev. B* **92** 134511
[95] Kihou K, Saito T, Fujita K, Ishida S, Nakajima1 M, Horigane K, Fukazawa H, Kohori Y, Uchida S, Akimitsu J, Iyo1 A, Lee C and Eisaki H *et al.* 2016 *J. Phys. Soc. Jpn.* **85** 034718
[96] Kihou K, Saito T, Ishida S, Nakajima M, Tomioka Y, Fukazawa H, Kohori Y, Ito T, Uchida S, Iyo A, Lee C H and Eisaki H 2010 *J. Phys. Soc. Jpn.* **79** 124713
[97] Wang A F, Zhou S Y, Luo X G, Hong X C, Yan Y J, Ying J J, Cheng P, Ye G J, Xiang Z J, Li S Y and Chen X H 2014 *Phys. Rev. B* **89** 064510
[98] Chen H, Ren Y, Qiu Y, Bao W, Liu R H, Wu G, Wu T, Xie Y L, Wang X F, Huang Q and Chen X H 2009 *Europhys. Lett.* **85** 17006
[99] Rotter M, Panger M, Tegel M and Johrendt D 2008 *Angew. Chem. Int. Edn.* **47** 7949
[100] Johrendt D, Hosono H, Hoffmann R and Pöttgen R 2011 *Z. Kristallogr.* **226** 435